Medical Imaging 2008: Ultrasonic Imaging and Signal Processing, edited by Stephen A. McAleavey, Jan D'hooge, Proc. of SPIE Vol. 6920, 692018, (2008) · 1605-7422/08/$18 · doi: 10.1117/12.770811

Although several methods have been proposed to segment US images, only a few techniques have focused on elasticity images. Fahey et al. proposed the application of a simple threshold to acoustic radiation force impulse elastograms [12] with good result in phantom materials due to the high contrast between the inclusion and the background. Techavipoo et al. [13] proposed a semi-automated segmentation algorithm of thermal lesions for compression elastography images. The algorithm was based on thresholding and morphological operations and was applied to in vitro RFA lesions. Later, an automated algorithm was reported by the same group [14]. The approach consisted of a coarse-to-fine method which was initialized by template matching and then refined by an active contour model. This technique was evaluated in 2D and 3D in vitro elastograms and a proof of concept was shown for 2D in vivo images.

interface. The evolving interface is obtained at any given time iteration by extrac

practice [20], an RFA lesion was created 1–2 cm beneath the liver surface. In the case of the HIFU experiments, a single-element focused transducer with a focal length of 6 cm and a diameter of 5cm (Model H-101, Sonic Concepts, Inc., Woodinville, WA, USA) was used. The focal intensity of the HIFU transducer is about 1000 W/cm^2. A continuous sinusoidal signal (frequency: 1.1 MHz, voltage: 0.95 V) produced from a function generator (Model 3511A Pragmatic Instruments, San Diego, CA, USA) was fed to a radiofrequency amplifier (Model 2100L, Electronic Navigation Industries, Rochester, NY, USA) which drove the transducer to generate the HIFU beams. The position of the HIFU transducer was adjusted to 4 cm above the liver surface. The water chamber was used as the acoustic coupling between the transducer and the liver surface. The bottom of the water chamber was made of an acoustic transparent film and adjusted to barely touch the liver surface. Within 20 seconds, a single lesion was created. Various-sized lesions were created in the liver by adjusting the duration of HIFU exposure.

Two pistons (Model 2706, Brüel & Kjaer, Naerum, Denmark) were applied directly on the surface of the liver to generate the vibration field needed for sonoelastography. Input signals to the vibration sources were produced by a harmonic waveform generator (Model 3511A Pragmatic Instruments, San Diego, CA, USA) after amplification (Model 2706, Brüel & Kjaer, Naerum, Denmark). The pistons were vibrated at a combination of low frequencies (105, 140, 175 and 210 Hz). Co-registered sonoelastographic and B-mode images were acquired using a linear probe array (M12L) connected to a Logiq 9 US scanner (General Electric Medical Systems, Milwaukee, WI, USA). The position and orientation of the probe over the liver was marked. After imaging, the pig was euthanized and the liver was excised. For

Matched sonoelastographic, B-mode and gross pathology images are presented in Fig. 1. A HIFU lesion is found at the top of the sonoelastographic image. The corresponding B-mode image shows a hyperechoic region due to the gas bubbles formed by the thermal process. The area of the hyperechoic region does not correspond to the area of the actual lesion. The gross pathology image confirms the presence of the lesion.

A comparison between manual and semi-automatic segmentation is illustrated in Fig. 2. Three independent observers manually drew different outlines for the same lesion. The same observers initialized the semi-automatic algorithm by choosing the center of the lesion. Even though they selected different centers, the algorithm produced the same outline.

5. DISCUSSION

[5] Zhang, M., "The measurement and imaging of viscoelastic properties of soft tissues and lesions," Ph.D. Dissertation, University of Rochester (2007).
[6] Hindley, J., Gedroyc, W.M., Regan, L., Stewart, E., Tempany, C., Hynyen, K., et al., "MRI guidance of focused ultrasound therapy of uterine fibroids: Early results," AJR. Am. J. Roentgenol., 183, 1713-1719 (2004).
[7] Cha, C.H., Lee, F.T., Gurney, J.M., Markhardt, B.K., Warner, T.F., Kelcz, F., et al., "CT versus sonography for monitoring radiofrequency ablation in a porcine liver," AJR. Am. J. Roentgenol. 175, 705-711 (2000).
[8] Varghese, T., Techavipoo, U., Liu, W., Zagzebski, J.A., Chen, Q., Frank, G., and Lee Jr., F.T., "Elastographic measurement of the area and volume of thermal lesions resulting from radiofrequency ablation: Pathologic correlation," AJR. Am. J. Roentgenol. 181, 701-707 (2003).
[9] Fahey, B.J., Hsu, S.J., Wolf, P.D., Nelson, R.C., and Trahey, G.E., "Liver ablation guidance with acoustic radition force impulse imaging: challenges and opportunities," Physics in Medicine and Biology, 51, 3785-3808 (2006).
[10] Lerner, R.M., Parker, K.J., Holen, J., Gramiak, R., and Waag, R.C., "Sonoelasticity: Medical elasticity images derived from ultrasound signals in mechanically vibrated targets," Acoust. Imaging, 16, 317-327 (1988).
[11] Huang, S.R., Lerner, R.M. and Parker, K.J., "On estimating the amplitude of harmonic vibration from the Doppler spectrum of reflected signals," J. Acoust. Soc. Am., 88, 310-317 (1990).
[12] Fahey, B.J., Dumont, D.M., and Trahey, G.E., "Volume visualization and error analysis using 3D ARFI Imaging Data," Proc. IEEE Ultrasonics symposium (2006).
[13]

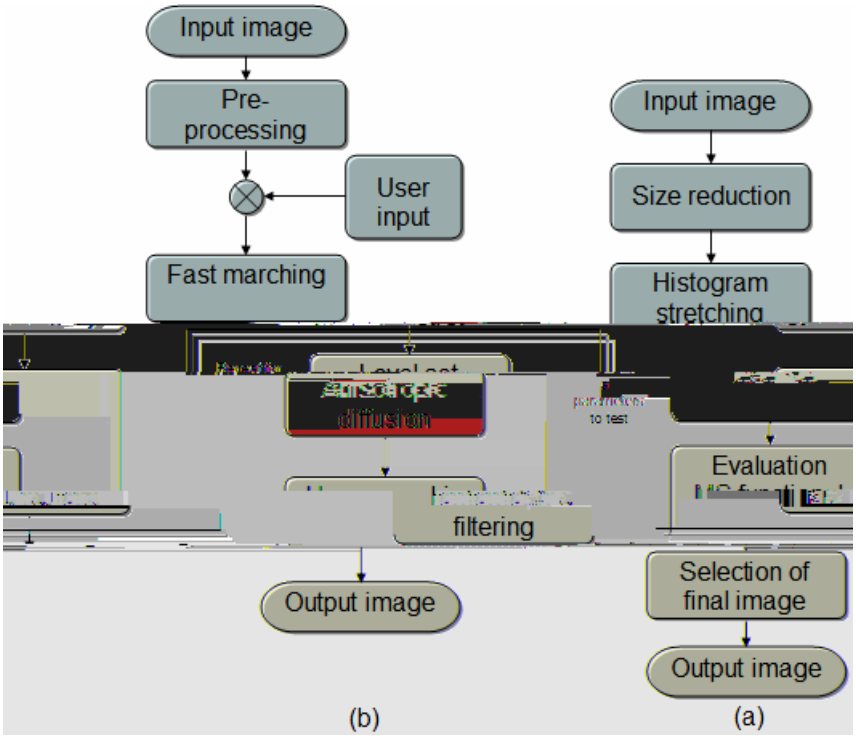

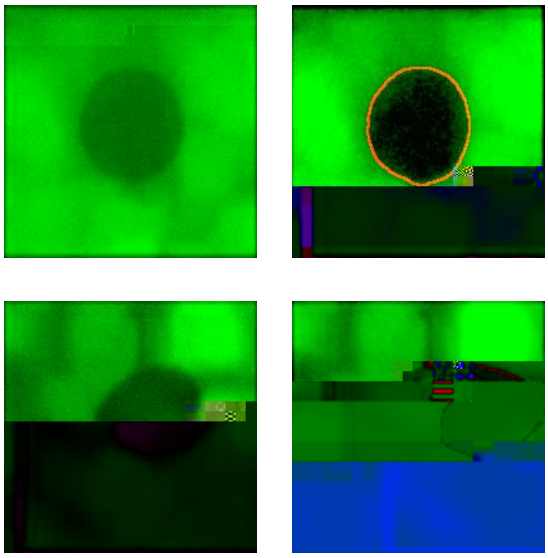

Table 1. Performance of the algorithm in terms of the percentage of overlap between the resulting segmentation and the ground truth for two simulated lesions.

	10% Contrast	20% Contrast	30% Contrast	40% Contrast
Lesion 1	92.3	94.3	96.4	96.9

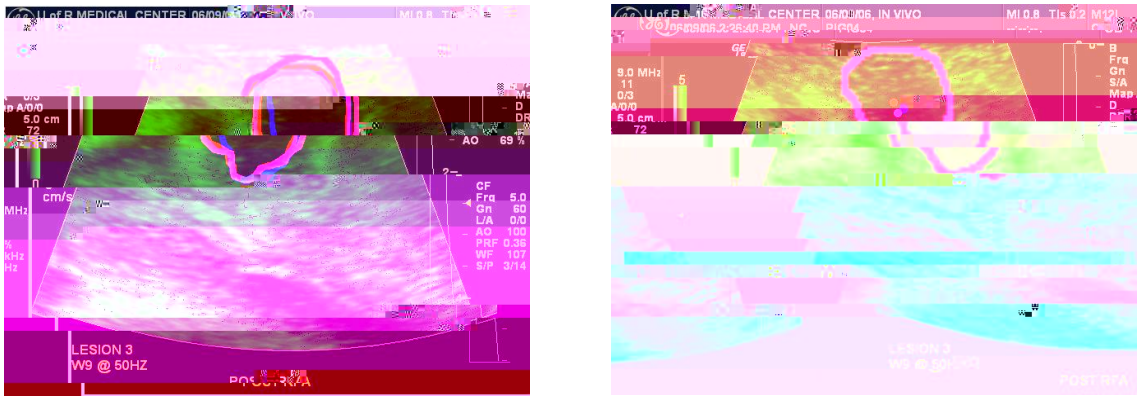

(a) (b)

Fig. 4. Comparison between (a) Manual and (b) Semi-automatic segmentation. Thr